# Static and Time-Resolved Fluorescence Studies of Fluorescent Phosphatidylcholine Bound to the Phosphatidylcholine Transfer Protein of Bovine Liver†

Theo A. Berkhout, Antonie J. W. G. Visser, and Karel W. A. Wirtz*

ABSTRACT: Phosphatidylcholine analogues containing a *cis*-parinaroyl chain at the *sn*-1, *sn*-2, or both *sn*-1 and *sn*-2 positions (1-PnA-PC, 2-PnA-PC, and diPnA-PC, respectively) have been used to investigate the lipid binding site of the phosphatidylcholine transfer protein (PC-TP) from bovine liver by fluorometric techniques. Binding of these fluorescent lipids to the protein was registered by measuring the enhancement of parinaroyl fluorescence and the quenching of the tryptophanyl fluorescence. The fluorescence intensity of 1-PnA-, 2-PnA- and diPnA-PC bound to PC-TP was proportional to the chromophore content. The energy-transfer efficiency between the tryptophan residues and the bound chromophores was approximately 40% for 1-PnA- and 2-PnA-PC and 60% for diPnA-PC. Quenching of the tryptophanyl fluorescence was, in part, accounted for by a decrease of the fluorescence lifetimes. The orientation of the 1 and 2 fatty acyl chains of the PnA-PC analogues on the transfer protein was analyzed by time-resolved fluorescence anisotropy measurements. The fluorescence anisotropy decayed according to a single exponential function yielding a rotational correlation time of 26 ns for 1-PnA-PC, 11 ns for 2-PnA-PC, and 15 ns for diPnA-PC. These correlation times indicate that both fatty acyl chains are immobilized at different positions on the protein. From the difference in correlation time we propose that the shape of the phosphatidylcholine transfer protein is ellipsoidal (axial ratio $\simeq$ 2.5) with the 1 fatty acyl chain oriented parallel to the long symmetry axis and having an angle of 60–90° with the 2 fatty acyl chain.

From the intracellular lipid-carrying proteins known to date, the phosphatidylcholine transfer protein (PC-TP)[1] from bovine liver is one of the best characterized (Wirtz, 1982). Its primary structure has been elucidated and shown to consist of a single polypeptide chain of 213 amino acid residues interconnected by two disulfide bridges (Akeroyd et al., 1981). As a specific carrier of PC between membranes, it forms a one-to-one molar complex (Demel et al., 1973). This makes PC-TP an attractive subject of investigation in those studies that aim for an understanding of principles that govern lipid–protein interactions.

Recently, the lipid binding site of PC-TP has been partially identified by covalent coupling of PC analogues containing photoactivable carbene precursors attached to the *sn*-2 fatty acyl chain (Westerman et al., 1983). Binding of PC analogues with nitroxide-labeled fatty acids at the *sn*-2 position demonstrated a strong interaction of the *sn*-2 fatty acyl chain with a hydrophobic cavity in the protein (Devaux et al., 1977; Machida & Ohnishi, 1978). Enzymatic and spectroscopic evidence indicated that the bound PC molecule was shielded from the medium (Kamp et al., 1975; Devaux et al., 1977).

In the present study, the nature of the lipid binding site on PC-TP is further investigated by use of PC containing *cis*-parinaric acid. Inherent to their very interesting spectroscopic properties, this and other conjugated polyene fatty acids are useful probes of membrane structure (Sklar et al., 1975, 1977a, 1979; Schroeder et al., 1976, 1983; Waring et al., 1979; Welti & Silbert, 1982) and lipid–protein interactions (Sklar et al., 1977b; Berde et al., 1979; Kimelman et al., 1979). In general, the absorption spectrum, fluorescence quantum yield, and lifetime are very sensitive to environment (Sklar et al., 1977c). Polarized, time-resolved fluorometric techniques allow one to determine fluorescence polarization anisotropy as a measure of acyl chain motion (Wolber & Hudson, 1981). Another attractive feature is the possibility of energy transfer between tryptophan residues and the parinaric acid chromophore in the lipid–protein complex (Sklar et al., 1977b; Kimelman et al., 1979), giving information on the sites of interaction.

Conjugated polyene fatty acids have been used to probe the fatty acid binding sites of bovine serum albumin (Sklar et al., 1977b). Here, we report on the binding of PC containing *cis*-PnA at the *sn*-1, *sn*-2, or both *sn*-1 and *sn*-2 positions to PC-TP as measured by static and time-resolved fluorescence methods. Application of these probe lipid molecules has demonstrated that the *sn*-1 and *sn*-2 fatty acyl chains of the bound PC molecule occupy different sites on PC-TP.

## Materials and Methods

*Materials.* *cis*-Parinaric acid (PnA) was purchased from Molecular Probes, Plano, TX, and egg phosphatidylcholine (PC), type III-E, from Sigma. Lysophosphatidylcholine (LPC) and phosphatidic acid (PA) were prepared from PC by treatment with phospholipase $A_2$ from *Crotalus adamanteus* (van den Bosch & van Deenen, 1965) and with phospholipase D from savoy cabbage (Davidson & Long, 1958), respectively. *N,N'*-Dicyclohexylcarbodiimide (DCC) and butylated hydroxytoluene (BHT) were obtained from Aldrich. 4-(Dimethylamino)pyridine (DMAP) and ethanol (fluorescent grade) were purchased from Merck. *sn*-Glycero-3-phosphocholine (GPC) as the $CdCl_2$ complex was a gift from R. Dijkman. Phosphatidylcholine transfer protein (PC-TP) was

† From the Laboratory of Biochemistry, State University of Utrecht, Padualaan 8, NL-3584 CH Utrecht, The Netherlands (T.A.B. and K.W.A.W.), and the Department of Biochemistry, Agricultural University, De Dreijen 11, NL-6703 BC Wageningen, The Netherlands (A.J.W.G.V.). *Received June 28, 1983.* This research was carried out under the auspices of The Netherlands Foundation for Chemical Research (S.O.N.) and with financial aid from The Netherlands Organization for the Advancement of Pure Research (Z.W.O.).

[1] Abbreviations: EDTA, ethylenediaminetetraacetic acid (disodium salt); Tris, tris(hydroxymethyl)aminomethane; BHT, butylated hydroxytoluene; DCC, *N,N'*-dicyclohexylcarbodiimide; DMAP, 4-(dimethylamino)pyridine; PnA, *cis*-parinaric acid; PC, phosphatidylcholine; LPC, lysophosphatidylcholine; DPPC, dipalmitoylphosphatidylcholine; PA, phosphatidic acid; GPC, *sn*-glycero-3-phosphocholine; PC-TP, phosphatidylcholine transfer protein; 1-PnA-PC, 1-parinaroyl-2-palmitoyl-*sn*-glycero-3-phosphocholine; 2-PnA-PC, 1-acyl-2-parinaroyl-*sn*-glycero-3-phosphocholine; diPnA-PC, 1,2-diparinaroyl-*sn*-glycero-3-phosphocholine; TLC, thin-layer chromatography.

0006-2960/84/0423-1505$01.50/0 

purified to homogeneity from bovine liver according to established procedures (Kamp et al., 1973; Wirtz et al., 1979). The protein, 0.3 mg/mL, was stored at −20 °C in 50% glycerol containing 10 mM sodium citrate–20 mM disodium hydrogen phosphate, pH 5.0. Silica gel was a product from Mallinckrodt, Sephadex G-25 from Pharmacia, and Bio-Gel A, 0.5 mesh, from Bio-Rad Laboratories. A mixed resin consisted of Bio-Rex 70 (4 mequiv/mL) and AG 3-X-4A (2 mequiv/mL) purchased from Bio-Rad Laboratories.

*Synthetic Procedures.* Chloroform was distilled over phosphorus pentoxide and stored on a 0.4-nm molecular sieve (Merck) under dry argon, just before use. Argon was dried over a column of 0.4-nm molecular sieve.

*cis*-Parinaroyl anhydride was prepared essentially as described by Selinger & Lapidot (1966). PnA (380 μmol) was dissolved in 1 mL of dry benzene (Merck) and rendered anhydrous by evaporation under argon. The reaction with DCC (190 mol) was carried out in 1 mL of chloroform for 4 h at room temperature. The mixture was filtered through a glasswool-stoppered Pasteur pipette into a reaction vial that contained anhydrous LPC (120 μmol) and DMAP (120 μmol), and 2-PnA-PC was formed (Gupta et al., 1977). At all stages of handling, the parinaroyl derivatives were kept under argon atmosphere and only exposed to green-yellow light (Philips PF 710). 2-PnA-PC was purified on a $SiO_2$ column, in chloroform/methanol (65:35 v/v), saturated with argon and containing BHT (5 μM) and characterized essentially as described by Somerharju et al. (1981). The yield was 110 μmol, i.e., 90%.

diPnA-PC was prepared by addition of *cis*-parinaroyl anhydride (190 μmol) to GPC–$CdCl_2$ adduct (60 μmol) and DMAP (120 μmol) in 1 mL of chloroform as described above. After 24 h, methanol (1.25 mL) and water (0.25 mL) were added, and the suspension was filtrated. The clear solution, containing BHT (5 μM), was passed through a column of mixed resin (100 mequiv/mequiv of DMAP) to remove DMAP and $CdCl_2$ from diPnA-PC (Gupta et al., 1977). After removal of the solvent by rotational evaporation, the residue was dissolved in chloroform under argon atmosphere. DiPnA-PC was purified on silica gel as described for 2-PnA-PC. The yield was 33 μmol (55%). DiPnA-PC showed a single spot on thin-layer chromatography (silica gel plate, F 254, Merck) with an $R_f$ value similar to that of egg PC (solvent was chloroform/methanol/ammonia/water, 90:55:5.5:5.5 v/v). The absorption spectrum in ethanol was identical with that of free PnA and showed no triene absorption in the 250-nm region (Gunstone, 1967). diPnA-PC contained 2.0 mol of PnA/mol of lipid phosphorus, assuming a molecular absorption coefficient of 78 000 at 306 nm in ethanol (Sklar et al., 1977c). Lipid phosphorus was determined by the method of Rouser et al. (1970).

diPnA-PC (8 μmol) was dissolved in 0.5 mL of ether and added to 0.5 mL of 0.1 M borate buffer (pH 7.4) containing $CaCl_2$ (0.25 mM) and 5 units of phospholipase $A_2$. The mixture was rotated under argon atmosphere at room temperature for 3 h. Additional ether (3 mL) was added and the ether layer containing most of the fatty acid removed. The aqueous layer was extracted according to Bligh & Dyer (1959). The extraction was repeated twice to fully recover the 1-PnA-LPC formed. The combined chloroform extracts were evaporated under argon flush. The lipid film was washed 3 times with 1 mL of anhydrous ether saturated with argon and containing 0.01% BHT, to remove traces of PnA. This extraction did not lead to losses of 1-PnA-LPC. The yield was 90%. 1-PnA-PC was prepared by acylation of 1-PnA-LPC and palmitoyl anhydride and purified as described above. 1-PnA-PC contained 0.97 mol of PnA/mol of phosphorus and migrated as a single spot on TLC. The absorption spectrum was identical with that of PnA. To check the position of the parinaroyl fatty acyl chain, 1-PnA-PC (0.5 μmol) was treated with phospholipase $A_2$. TLC on the reaction products showed that only the LPC spot was fluorescent. Furthermore, 1-PnA-LPC isolated as described above contained 0.93 mol of PnA/mol of phosphorus.

The PnA-PC derivatives were dissolved in ethanol (1–4 mM, 1–5 mol % BHT) and stored in dark brown bottles fitted with Teflon caps at −40 °C under argon atmosphere. The solutions were stable under these conditions. Before use, the PnA-PC derivatives were routinely checked by measuring their absorption spectra.

*Preparation of Phospholipid Vesicles.* Vesicles consisting of PnA-PC derivatives were prepared by the ethanol injection technique (Batzri & Korn, 1973). Ethanolic solutions of PnA-PC (1–4 mM) were directly injected into 20 mM Tris-HCl, 5 mM EDTA, and 100 mM NaCl buffer, pH 7.4 (TES buffer). The buffer was degassed under vacuum and saturated with argon for 30 min before use. The amount of injected ethanol did not exceed 0.5% (v/v). Vesicles of nonfluorescent phospholipids were prepared by sonication. Phospholipid (1–10 mM) was dispersed in 2 mL of TES buffer and ultrasonically irradiated by a Branson sonifier (60 W, 10 min) in ice under a stream of nitrogen. The vesicles were centrifuged at 45 000 rpm for 60 min in a Beckman rotor to remove titanium particles, dust, and multilamellar structures. Prior to use, BHT (1–5 mol %) was added to the preparations.

*Preparation of the Parinaroyl-PC–Transfer Protein Complex.* PnA-PC was bound to PC-TP by addition of 1 mL of PC-TP solution (0.3 mg in 50% glycerol) to 2 mL of TES buffer containing ethanol-injection vesicles (100 nmol of PnA-PC). The mixture was kept under argon atmosphere in the dark at room temperature and rotated for 60 min. The PnA-PC–PC-TP complex was separated from the vesicles by molecular sieve chromatography on a column (20 × 0.6 cm) of Sephadex G-25. This column had been prewashed with sodium deoxycholate (2% w/v) followed by extensive washing with argon-saturated TES buffer. The PnA-PC–PC-TP complex was recovered in the void volume while the vesicles were retained on the column by absorption. In some instances, the PnA-PC–PC-TP complex was isolated by chromatography on a Bio-Gel A, 0.5M, column (Moonen et al., 1979). Concentration of native PC-TP was determined by measuring the absorbance at 280 nm ($\epsilon$ = 60 365 $M^{-1}$ $cm^{-1}$).

*Fluorescence Experiments.* Static fluorescence experiments were carried out at 25 °C on a Perkin-Elmer MFP-3 fluorometer equipped with a thermostatic cuvette holder. During measurements, the contents of the cuvette were continuously mixed by a magnetic stirrer. The PC-TP-mediated transfer of PnA-PC derivatives between donor vesicles prepared of pure PnA-PC and unlabeled acceptor vesicles was spectrofluorometrically monitored as described by Somerharju et al. (1981). The spectra were recorded in the ratio mode. Excitation was at 324 nm (slit 2 nm) and emission at 420 nm (slit 40 nm). Binding of PnA-PC to PC-TP was measured by titration of self-quenched vesicles consisting of pure PnA-PC in 2 mL of TES buffer with PC-TP. Binding gave an increase of parinaroyl fluorescence intensity, which was recorded at 420 nm as above. Corrections for the contribution of tryptophanyl fluorescence were made. Under the conditions of titration, the fluorescence of the vesicles remained fully quenched (see Results). Quenching of tryptophanyl fluorescence by PnA-PC

derivatives was measured by direct injection of an ethanolic solution of PnA-PC into the cuvette containing PC-TP (1 nmol) in 2 mL of TES buffer. The final concentration of ethanol in the solution did not exceed 1% (v/v) and had no effect on the measurements. The emission spectra (slit 20 nm) were recorded in the direct mode (excitation at 255 nm, slit 10 nm) and corrected for the contribution by PnA-PC vesicles. The spectra were not corrected for inner and outer filtering effect, since the optical density at the emission and excitation wavelength was below 0.1.

Time-resolved, polarized fluorescence measurements were performed at 20 °C with the set-up previously described (van Hoek et al., 1983). For the measurement of protein fluorescence decay, a double monochromator in the detection light path was used, while excitation was at 294 nm. For parinaroyl fluorescence, the excitation was at 305 nm, the emission was viewed through a Schott KV399 barrier filter, and the set-up was used with Glan-Thompson polarizers. The data for tryptophan fluorescence were accumulated for 5 min, whereas the impulse response function required about 1-min sampling time. The fluorescence and anisotropy decay of the PnA-PC derivatives were obtained via a repeated cycle of measuring the parallel ($I_\parallel$) and perpendicular ($I_\perp$) fluorescent components, each for 10 s. Ten cycles were usually sufficient for a good signal to noise ratio. Background was subtracted from the fluorescence data, because blanks were measured in the same way as the fluorescent samples (optical density at excitation wavelength < 0.1). For protein fluorescence, the blank was the buffer used, while for parinaroyl-containing samples the same amount of protein or lipid without the fluorescent dye was used for subtraction. Four cycles of collecting the impulse response function were sufficient, and the pulses measured before and after the fluorescence data were averaged and used for deconvolution procedures. The 512 data points of each component were stored into subgroups of an 8K memory of a multichannel analyzer (ND66, Nuclear Data). Stored data were transferred via communication linkage to the DEC-10 computer of the Agricultural University, where the actual data processing and decay analysis took place. Fluorescence and anisotropy decays were analyzed via a nonlinear least-squares iterative procedure. Elements of this procedure have been described in previous publications (van Hoek et al., 1983; Visser, 1982; Papenhuijzen & Visser, 1983). For parinaroyl fluorescence decay, the following expression was used:

$$S(t) = I_\parallel(t) - I_\parallel^B(t) + 2[I_\perp(t) - I_\perp^B(t)]$$

where $I_\parallel(t)$ and $I_\perp(t)$ are the time-dependent polarized emission components and the superscript B denotes the intensity components arising from the blank. For time-dependent anisotropy, we used $r(t) = D(t)/S(t)$, where $D(t) = I_\parallel(t) - I_\parallel^B(t) - [I_\perp(t) - I_\perp^B(t)]$.

## Results

*Transfer of cis-Parinaroyl-PC Derivatives to Vesicles.* In previous studies, we have shown that vesicles consisting of pure 2-PnA-PC have a very low fluorescence intensity due to self-quenching of the probe molecules (Somerharju et al., 1981, 1983). Dilution of PnA-PC with unlabeled PC, prior to vesicle formation, interfered with effective probe–probe interactions, thereby enhancing the fluorescence intensity. Vesicles displayed a maximal fluorescence when the PnA-PC content did not exceed 5 mol % (Somerharju et al., 1983). This forms the basis for the continuous spectrofluorometric assay where transfer of PnA-PC is measured between donor vesicles consisting of pure PnA-PC and acceptor vesicles of unlabeled

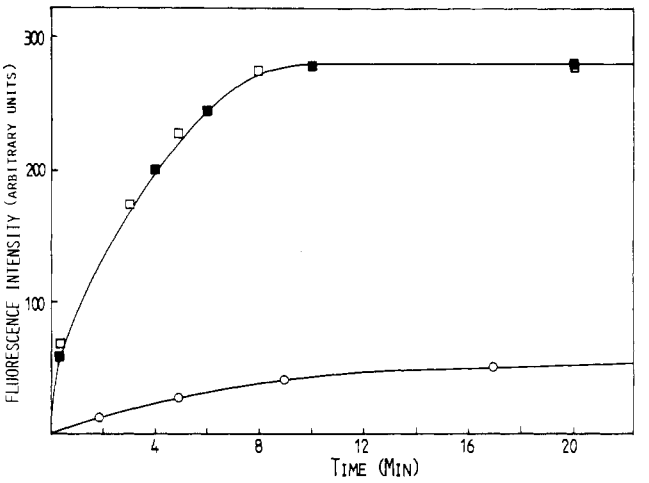


FIGURE 1: Transfer of PnA-PC analogues from donor to acceptor vesicles as catalyzed by the phosphatidylcholine transfer protein. The donor vesicles consisted of 1-PnA-PC (8 nmol of lipid phosphorus), 2-PnA-PC (8 nmol of lipid phosphorus), and diPnA-PC (4 nmol of lipid phosphorus) and the acceptor vesicles of egg PC-PA (80:20 mol %, 200 nmol of lipid phosphorus). The transfer reaction was started by addition of PC-TP (0.1 nmol) in 2 mL of TES buffer at 25 °C. (□) 1-PnA-PC; (■) 2-PnA-PC; (○) diPnA-PC.

phospholipids. In this study, donor vesicles prepared of 1-PnA-PC, 2-PnA-PC, or diPnA-PC (8 nmol of PnA chromophore) were mixed with an excess (200 nmol of lipid phosphorus) of acceptor vesicles consisting of egg PC–PA (80:20 mol %). Under these conditions, the fluorescence intensity (emission at 420 nm) remained very low with time of incubation, indicating a lack of spontaneous transfer of PnA-PC from the donor to the acceptor vesicles. Upon addition of PC-TP, the fluorescence intensity increased with time due to the protein-mediated transfer of PnA-PC to the acceptor vesicles. As is shown in Figure 1, 1-PnA-PC and 2-PnA-PC were transferred at an equal rate, suggesting that PC-TP has no preference for either species of PC. Equilibrium is attained within 10 min, at which time the fluorescence intensity is approximately 60% of that observed for 1-PnA-PC and 2-PnA-PC, premixed with the acceptor phospholipids. This indicates that PC-TP maximally transfers 60% of the donor PnA-PC pool. In agreement with previous observations, this pool most likely constitutes the outer monolayer of the donor vesicles (Johnson et al., 1975; Rothman & Dawidowitz, 1975).

Premixing of diPnA-PC (8 nmol of PnA chromophore) with the acceptor phospholipids (200 nmol of lipid phosphorus) yielded 30% of the fluorescence intensity observed with 1- and 2-PnA-PC (8 nmol of PnA chromophore). This may indicate a substantial probe–probe interaction on the diPnA-PC molecule embedded in the vesicle bilayer. From Figure 1, it follows that PC-TP transfers diPnA-PC to the acceptor vesicles as well. If we take into account the difference in fluorescence yield with respect to 1- and 2-PnA-PC, transfer of diPnA-PC will be expected to level off at a maximal fluorescence intensity of approximately 80, i.e., 30% of 280 arbitrary units. It is evident that, in contrast to 1- and 2-PnA-PC, the equilibrium for diPnA-PC is still not attained after 20 min of incubation. From this and other experiments measuring the initial rates, we have estimated that PC-TP transfers diPnA-PC at about half the rate observed for 1- and 2-PnA-PC (results not shown).

*Binding of PnA-PC Derivatives to PC-TP by Enhanced Fluorescence.* Transfer implies that PC-TP forms a complex with the probe molecules. Complex formation was measured directly by titration of vesicles prepared of pure 2-PnA-PC (2 nmol) with PC-TP. As shown in Figure 2A, the fluores-

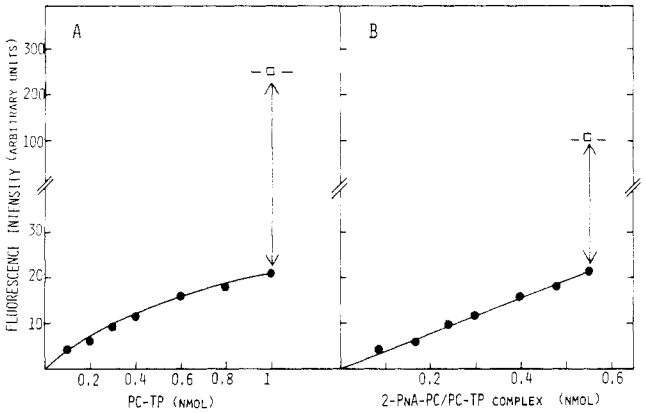


FIGURE 2: Binding of 2-PnA-PC to phosphatidylcholine transfer protein. (A) Vesicles of 2-PnA-PC (2 nmol of lipid phosphorus) in 2 mL of TES buffer were titrated with PC-TP, and the increase of fluorescence intensity was plotted as a function of protein concentration (●). Upon addition of 1 nmol of PC-TP, an excess of acceptor vesicles (200 nmol of egg PC-PA, 80:20 mol %) was added (□). (B) In the titration of a fixed amount of vesicles (2 nmol of lipid phosphorus), only PnA-PC of the outer monolayer (i.e., 1.2 nmol) is available for exchange with PC-TP. At complete equilibration with the endogenous PC molecule, the amount of 2-PnA-PC–PC-TP complex ($z$) formed follows from the equation: $z = x[y/(x + y)]$ where $x$ is the nanomoles of outer monolayer 2-PnA-PC and $y$ the nanomoles of PC-TP added (●). The fluorescence intensity upon addition of an excess of vesicles (see panel A) was corrected for the actual amount of 2-PnA-PC bound to PC-TP (□). In this instance, 0.55 nmol of 2-PnA-PC was transferred to the vesicles as compared to 1.2 nmol in (A).

cence intensity increased upon addition of PC-TP, indicating that self-quenching is abolished due to binding of 2-PnA-PC to the protein. Binding represents the exchange of the endogenous PC molecule bound to the protein and the 2-PnA-PC molecules present in the outer monolayer of the donor vesicles (i.e., 60% of 2 nmol). Under the conditions of titration, the dilution of PnA-PC in the vesicles by unlabeled PC from the protein did not exceed 40%. At this dilution, the fluorescence of the vesicles is still fully quenched (Somerharju et al., 1983). Hence, the increase of fluorescence measured is solely due to the binding of PnA-PC to PC-TP. Titration was continued up to 1 nmol of PC-TP, at which the fluorescence intensity equaled 21 arbitrary units (Figure 2A). Subsequent addition of an excess of acceptor vesicles (200 nmol of lipid phosphorus) further increased the fluorescence intensity to 259 arbitrary units. The final fluorescence intensity represents the incorporation of 1.2 nmol of 2-PnA-PC, originally available from the donor vesicles, into the acceptor vesicles. This level of fluorescence is identical with that attained by directly measuring the PC-TP-mediated transfer of 2-PnA-PC from donor to acceptor vesicles in the regular assay (data not shown).

For each PC-TP concentration, one can calculate the actual number of PC-TP molecules that contain a 2-PnA-PC molecule (see legend to Figure 2). This calculation presumes a complete equilibration of endogenous PC bound to PC-TP and the 2-PnA-PC pool, representing the outer vesicle monolayer (Westerman et al., 1983). If one plots the calculated nanomoles of 2-PnA-PC–PC-TP complex against the measured fluorescence intensities, a linear relationship is obtained in accordance with the presupposition of complete equilibration (Figure 2B). Upon addition of 1 nmol of PC-TP, 0.55 nmol of 2-PnA-PC is bound to the protein. Incorporation of this amount of 2-PnA-PC into the acceptor vesicles would yield a fluorescence intensity of 115 instead of 250 arbitrary units (see legend to Figure 2B). This shows that 2-PnA-PC has an approximately 5 times higher fluorescence intensity when it is incorporated in vesicles than bound to PC-TP. This difference in fluorescence yield has been confirmed by measuring lifetimes (see below).

Table I: Fluorescence Intensity of PnA-PC Derivatives in PC-TP and Egg PC Vesicles

| lipid | fluorescence intensity (arbitrary units)[a] | | |
|---|---|---|---|
| | PC-TP | vesicles | PC-TP/vesicles |
| 1-PnA-PC | 38 | 209 | 0.18 |
| 2-PnA-PC | 38 | 209 | 0.18 |
| diPnA-PC | 76[b] | 131 | 0.59 |

[a] The fluorescence intensities have been derived from Figure 2B by extrapolating to 1 nmol of PnA-PC bound to 1 nmol of PC-TP or incorporated into excess vesicles (200 nmol of lipid phosphorus). [b] This figure could not be determined directly, because of the incomplete equilibration of diPnA-PC with PC-TP. It was estimated to be twice the figure of 1- and 2-PnA-PC, as the ratio of absorption at 324 nm over emission at 420 nm was identical for each isolated PnA-PC–PC-TP complex.

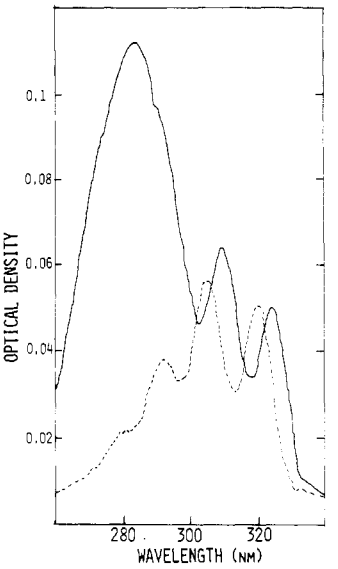


FIGURE 3: Absorption spectrum of 2-PnA-PC bound to phosphatidylcholine transfer protein (—) and in ethanol (– –). The 2-PnA-PC–PC-TP complex was isolated by molecular sieve chromatography on Bio-Gel A, 0.5 mesh.

Similar experiments have been performed with 1-PnA-PC and diPnA-PC. 1-PnA-PC behaved identical with 2-PnA-PC. In agreement with the slower transfer between vesicles (see Figure 1), we observed that diPnA-PC bound less readily to PC-TP than 1- and 2-PnA-PC. The estimated fluorescence intensities of 1-, 2-, and diPnA-PC (1 nmol) in PC-TP and in vesicles are presented in Table I. It is of great interest that diPnA-PC in PC-TP has double the fluorescence intensity of 1- and 2-PnA-PC, indicating that self-quenching does not occur. Self-quenching of this probe molecule does occur in the vesicles where the fluorescence intensity of diPnA-PC is 60% (corrected for the chromophore content only 30%) of that observed for 1- and 2-PnA-PC.

The absorption spectrum of the 2-PnA-PC–transfer protein complex isolated by molecular sieve chromatography is given in Figure 3. For comparison, we have also included the spectrum of 2-PnA-PC in ethanol. It is evident that the maxima of the vibronic bands of the bound chromophore are slightly red-shifted (310 and 324 nm). The spectra of 1- and diPnA-PC bound to PC-TP displayed identical characteristics. Emission spectra of the PnA-PC–PC-TP complexes have been determined as well. The ratio of emission intensity at 420 nm over absorption intensity at 324 nm was very similar for all three PnA-PC derivatives bound to PC-TP, implying a similar

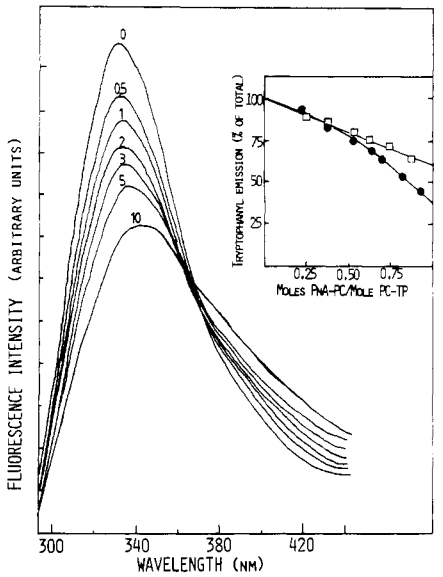


FIGURE 4: Fluorescence emission spectrum of phosphatidylcholine transfer protein in the presence of 2-PnA-PC. The PC-TP concentration was $0.5 \times 10^{-6}$ M. Excitation was at 255 nm (band width 10 nm), and the emission was measured at a band width of 20 nm. The numbers refer to the nanomoles of vesicle 2-PnA-PC added. (Insert) Moles of PnA-PC–PC-TP complex formed are plotted against the residual tryptophanyl fluorescence. See legend to Figure 2 for calculation of amount of complex formed. 2-PnA-PC (□); diPnA-PC (●).

quantum yield for all three probes.

*Quenching of Tryptophanyl Fluorescence on Binding of PnA-PC.* Binding of PnA-PC derivatives to PC-TP was also determined by monitoring the tryptophanyl fluorescence spectrum. Tryptophan was excited at 255 nm to avoid direct excitation of PnA-PC. Addition of increasing amounts of 1-PnA-PC vesicles to PC-TP resulted in a progressive decrease of tryptophanyl fluorescence intensity (Figure 4). This reflects a radiationless energy transfer between tryptophan residue(s) and 1-PnA-PC bound to PC-TP. The extent to which 1-PnA-PC is bound to PC-TP is governed by the exchange mechanism described above (see legend to Figure 2). For example, upon addition of 5 nmol of vesicle 1-PnA-PC, 1 nmol of PC-TP contains 0.75 nmol of 1-PnA-PC. In Figure 4 (insert), tryptophanyl fluorescence intensity is plotted against the calculated moles of 1-PnA-PC per mole of PC-TP. It appears that there is a linear relationship between tryptophanyl fluorescence quenching and the concentration of 1-PnA-PC on the protein. Upon extrapolation to PC-TP being fully loaded with 1-PnA-PC, tryptophanyl fluorescence is quenched approximately 40%. On binding, the emission maximum shifts from 329 to 335 nm. This slight red-shift may indicate that energy transfer occurs between the more apolar tryptophan residues and 1-PnA-PC (Burstein et al., 1973). Addition of 2-PnA-PC had essentially the same effect on the tryptophanyl fluorescence as 1-PnA-PC. Doubling of the chromophore content by binding of diPnA-PC to PC-TP resulted in an enhanced quenching to a value of 60%. However, there was no linear relationship between the tryptophanyl quenching and the theoretical amount of diPnA-PC bound (see insert to Figure 4). This probably reflects the relatively low affinity of PC-TP for diPnA-PC, resulting in an incomplete molecular exchange at low diPnA-PC vesicle concentrations. In accordance with the exchange mechanism, quenching of PC-TP was abolished when an excess (50 nmol) of egg PC was subsequently added.

*Tryptophanyl Fluorescence Decay.* In order to study in more detail the quenching of tryptophanyl fluorescence by the PnA-PC derivatives, we have determined the fluorescence decay of PC-TP. The tryptophanyl fluorescence decay of native PC-TP is shown in Figure 5. This fluorescence decay is nonexponential; the best fit is obtained with a sum of three exponential terms reflecting the composite decay (Table II). Complex kinetics were to be expected since PC-TP contains five tryptophan residues (Akeroyd et al., 1981). Binding of the PnA-PC derivatives resulted in energy transfer from the tryptophan residues to the chromophoric lipid (cf. Figure 4). The fluorescence decay of the 2-PnA-PC–PC-TP complex resembled closely that of PC-TP (cf. Figure 5). As shown in Table II, the longer lifetime components are unaffected by the presence of the chromophore. However, the short lifetime component that contributes 50–60% to the decay, declines from 0.8 to 0.4 ns, indicating the occurrence of a small amount of energy transfer. The relative contribution of the short lifetime component to the total fluorescence of native PC-TP is on the order of 27% (obtained by calculating $\alpha_1\tau_1/\sum_{i=1}^{3}\alpha_i\tau_i$; cf. Table II). This number decreases to 13% after binding 2-PnA-PC. According to this analysis, quenching of tryptophanyl fluorescence is distinctly less than that observed with static fluorescence (cf. Figure 4; see also Discussion).

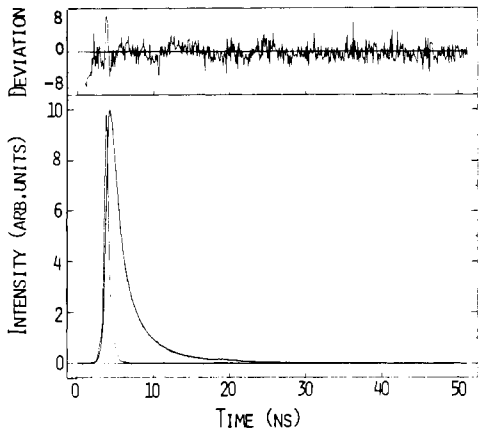


FIGURE 5: Fluorescence decay of tryptophan residues in PC-TP. The time evolution of three curves is shown: the spike-shaped exciting laser pulse $g(t)$, the experimental fluorescence $S(t)$, and the convolution product $S_c(t) = \int_0^t g(t - t')F(t')\,dt'$. $F(t)$ is the assumed decay function, in this case $F(t) = \sum_{i=1}^{3}\alpha_i \exp(-t/\tau_i)$. The parameters $\alpha_i$ and $\tau_i$ were varied until the best fit was obtained. The parameters are listed in Table II, in which the most significant digit indicates the standard error involved. For instance, 5.0 ns indicates that the standard error is within 0.1 ns. The deviation function, shown in the top panel, is the weighted residual value in each time channel, $[S(t) - S_c(t)]/[S(t)]^{1/2}$. A normal distribution of this function around zero indicates a good fit. For this particular example, the peak channels contained 18 097 fluorescence counts and 98 434 counts of the laser pulse. After normalization to 10 000 counts, $\chi^2 = 1.00$ in this case.

Table II: Fluorescence Decay Characteristics of PC Transfer Protein and Parinaroyl-PC Derivatives

| sample | $\alpha_1$ | $\tau_1$ (ns) | $\alpha_2$ | $\tau_2$ (ns) | $\alpha_3$ | $\tau_3$ (ns) |
|---|---|---|---|---|---|---|
| Tryptophanyl Fluorescence Decay | | | | | | |
| PC-TP | 0.57 | 0.8 | 0.35 | 2.3 | 0.07 | 5.7 |
| 2-PnA-PC–PC-TP | 0.52 | 0.4 | 0.37 | 2.0 | 0.11 | 5.6 |
| Parinaroyl Fluorescence Decay | | | | | | |
| 2-PnA-PC (ethanol) | 0.99 | 2.0 | 0.01 | 8.1 | | |
| 2-PnA-PC (*n*-decane) | 1.00 | 5.3 | | | | |
| 2-PnA-PC (egg PC vesicles) | 0.46 | 2.5 | 0.54 | 7.7 | | |
| 2-PnA-PC–PC-TP | 0.88 | 1.7 | 0.12 | 8.7 | | |
| 1-PnA-PC–PC-TP | 0.86 | 1.1 | 0.14 | 8.5 | | |
| diPnA-PC–PC-TP | 0.80 | 1.4 | 0.20 | 8.4 | | |

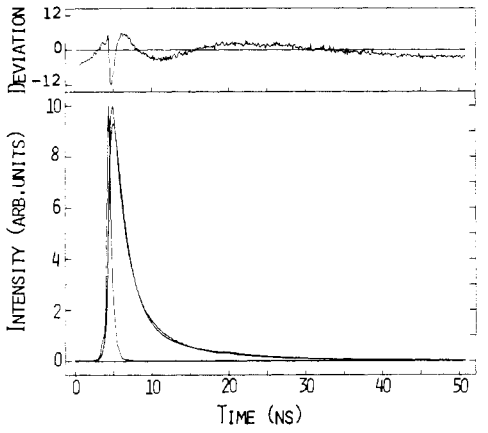


FIGURE 6: Fluorescence decay of 2-PnA-PC bound to PC-TP. For explanatory details, see the legend of Figure 5. Note from the course of the deviation function that the analysis into two lifetime components did not result in an optimum fit ($\chi^2 = 5.8$ after normalization in this case). For close comparison among the three PnA-PC derivatives used, a two-component analysis is preferred, and the results are listed in Table II. The peak excitation channel contained 129 982 counts; the fluorescence response had 63 799 counts in the peak.

*Parinaroyl-PC Fluorescence Decay.* We have measured the fluorescence decay of 2-PnA-PC in single solvents, incorporated in vesicles, and bound to PC-TP. As a typical example, the fluorescence decay of 2-PnA-PC bound to PC-TP is shown (Figure 6). The experimental data for ethanol and *n*-decane could be fitted with a single lifetime of fluorescence, 2.0 and 5.3 ns, respectively (Table II). These values are in excellent agreement with those of Sklar et al. (1977c) and reflect the great sensitivity of the lifetimes for solvent polarity. Both for 2-PnA-PC present in vesicles and PC-TP, the fluorescence decay has to be described minimally by a sum of two exponential terms. In egg PC vesicles we have an equal contribution of a short (2.5-ns) and long (7.7-ns) lifetime component. In PC-TP, we have a predominant combination (≈85%) of a short lifetime component of 1.7 ns and a distinctly longer component (8.7 ns). Slight variations in these values were observed when 1-PnA-PC and diPnA-PC were bound to PC-TP (Table II). The predominance of the short lifetime component in PC-TP is reflected in the much lower fluorescence yield observed in PC-TP as compared to vesicles (see Figure 2).

*Parinaroyl-PC Fluorescence Anisotropy Decay.* The dynamic fluorescence behavior of the lipid probes in vesicles and PC-TP was further analyzed by determining the anisotropy. As an example, the time-dependent fluorescence depolarization of 2-PnA-PC in vesicles and PC-TP is presented in Figure 7. As has been observed by Wolber & Hudson (1981) for PnA-PC in dipalmitoyl-PC vesicles above the transition temperature, the anisotropy decay of 2-PnA-PC in egg PC vesicles is characterized by a short decay (correlation time of 1.9 ns) and a relatively long lifetime component (correlation time of 35 ns). The short decay represents a rapid restricted motion of large amplitude superimposed on an immobilized part, reflecting the rotation of the vesicle. The anisotropy decay of 2-PnA-PC in PC-TP was a single exponential function in the time range of observation, i.e., 10 ns (see Figure 7B). A similar behavior was observed for 1-PnA-PC and diPnA-PC in PC-TP. The key data are summarized in Table III. The rotational correlation times for 2-PnA-PC and 1-PnA-PC are 11 and 26 ns, respectively. Both the high initial anisotropy (at $t = 0$; see Figure 7B) and the relatively long correlation times indicate that the chromophores are tightly bound to PC-TP. The difference in correlation times strongly suggests that the *sn*-1 and *sn*-2 fatty acyl chains have their own, specific orientation

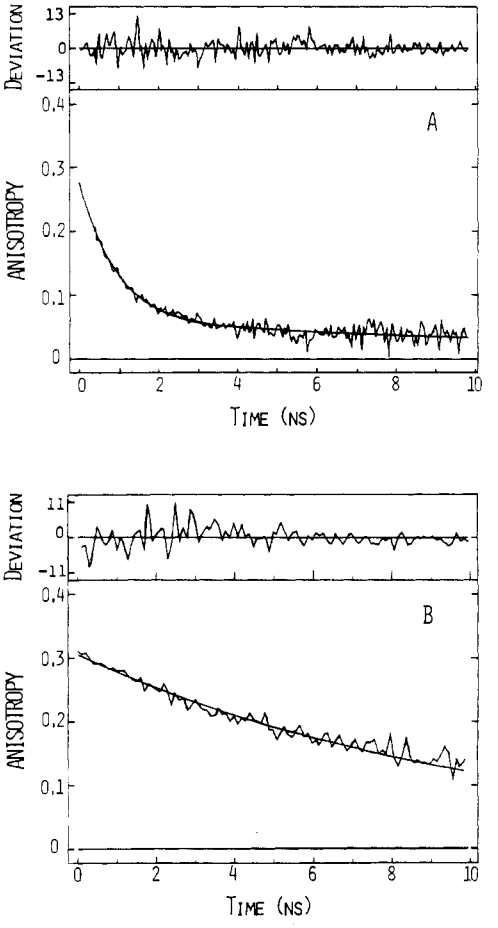


FIGURE 7: Fluorescence anisotropy decay of 2-PnA-PC in egg PC vesicles (A) and bound to PC-TP (B). The experimental anisotropy $r(t)$ is represented by the noisy curve, and analysis started at the maximum of the exciting laser pulse (not shown). The smooth line is the fitted decay function, which is a double exponential for the vesicle system and a single exponential for the PC-TP-bound fluorophore. The short correlation time (1.9 ns) is characteristic for a rapid restricted motion of 2-PnA-PC within the vesicle superimposed on the overall vesicle rotation. As reflected by the large amplitude, the system is above the phase transition temperature. All parameters ($\beta_i$, $\phi_i$) have been listed in Table III, where the most significant digit (as for the lifetimes) is characteristic for the standard error involved; for example, $\phi = 11$ ns has a standard error within 1 ns. The top panel contains the weighted residual in each time channel, $[r(t) - r_c(t)] + \omega(t)$, where the weighting factor is given by $\omega(t) = 1/[v(t)]^{1/2}$ and $v(t)$ is the variance of $r(t)$ (Wahl, 1979). Note also that from the deviation function only the initial part of the decay is of relevance in the case of PC-TP-bound 2-PnA-PC, since the average fluorescence lifetime is rather short.

Table III: Rotational Anisotropy Decay of Parinaroyl-PC Derivatives[a]

| sample | $\beta_1$ | $\phi_1$ (ns) | $\beta_2$ | $\phi_2$ (ns) |
|---|---|---|---|---|
| 2-PnA-PC (egg PC vesicles) | 0.25 | 1.9 | 0.01 | 35 |
| 2-PnA-PC-PC-TP | 0.31 | 11 | | |
| 1-PnA-PC-PC-TP | 0.31 | 26 | | |
| diPnA-PC-PC-TP | 0.31 | 15 | | |

[a] $\phi$ is the rotational correlation time; $\beta_1 + \beta_2$, anisotropy of $t = 0$.

on the protein. This difference is not compatible with a spherically shaped protein (see Discussion). With bound diPnA-PC, the characteristic correlation time is intermediate between those of 1- and 2-PnA-PC (i.e., 15 ns). This correlation time agrees very well with the harmonic mean $\langle\phi\rangle = 2\phi_1\phi_2/(\phi_1 + \phi_2)$, where $\phi_1$ and $\phi_2$ are the correlation times of 1- and 2-PnA-PC, respectively. This strongly suggests that

the two chromophores are independently photoselected and behave as isolated probes.

## Discussion

In this paper we have investigated the binding of various PnA-PC derivatives to bovine liver PC-TP by both static and time-resolved fluorescence measurements. Attention was focused on the relationship between tryptophan fluorescence and the occurrence of energy transfer to the bound PnA-PC molecule. In addition, we have determined fluorescence lifetimes and rotational correlation times of PnA-PC bound to PC-TP.

Both from the transfer experiments (Figure 1) and the titration studies (Figure 2), it is evident that PC-TP readily forms a complex with 1-PnA-PC and 2-PnA-PC. Binding of diPnA-PC was slower, probably due to the more rigid structure of the two fatty acyl chains. In a previous study, the fatty acid binding sites of bovine and human serum albumin were investigated by use of conjugated polyene fatty acids (Sklar et al., 1977b; Berde et al., 1979). Binding of these fatty acids to bovine serum albumin resulted in quenching of tryptophan fluorescence, which was attributed to Förster-type energy transfer. Similarly, the tryptophan fluorescence was partially quenched by binding of 1-PnA-, 2-PnA-, and diPnA-PC. The degree of quenching upon binding of 1 mol of 1-PnA-PC (2-PnA-PC)/mol of PC-TP was about 40% (Figure 4). This compares favorably with the energy-transfer efficiency of 30%, on binding of 1 nmol of *cis*-PnA/mol of bovine serum albumin (Sklar et al., 1977b). Here we need to take into account the presence of five tryptophan residues in PC-TP as compared to two residues in bovine serum albumin. On the other hand, the single tryptophan residue of the M13 coat protein, reconstituted in dimyristoyl-PC vesicles, was found to be very efficiently quenched by addition of parinaric acid, i.e., energy-transfer efficiency of about 60% for 1 mol of PnA/3 mol of tryptophan (Kimelman et al., 1979).

Binding of diPnA-PC lowered the tryptophanyl fluorescence intensity of PC-TP more effectively than 1- and 2-PnA-PC (see insert of Figure 4). This shows that energy transfer in PC-TP can be rather efficient, suggesting a favorable orientation of the chromophores involved. On the other hand, the very slight effect of the 2-PnA-PC chromophore on the lifetimes of the tryptophanyl fluorescence indicates a lack of efficient energy transfer (see Table II). From the fluorescence-decay results, it can be estimated that the energy transfer is about half of that observed by static fluorescence measurements. This discrepancy may, in part, be explained by the fact that the static fluorescence was measured by excitation at 255 nm and the dynamic fluorescence by excitation at 295 nm. At 255 nm, direct excitation and tyrosin-sensitized excitation contribute to the tryptophanyl fluorescence. Direct energy transfer from tyrosin (a total of 15 residues) to PnA-PC will compete with the excitation of tryptophan, thus leading to additional quenching of tryptophanyl fluorescence. An excitation of 255 nm was selected to avoid light absorption by PnA-PC. In the fluorescence decay experiments, excitation at 295 nm is allowed as light absorption by PnA-PC does not affect the kinetic behavior of tryptophanyl fluorescence decay. Detailed interpretation of the quenching by PnA-PC is not possible because of the relatively large number of tryptophan residues present in PC-TP. This is further complicated by the complex fluorescence decay kinetics of tryptophan itself (Szabo & Rayner, 1980).

The lipid binding of PC-TP was probed by PnA-PC derivatives. From the static fluorescence measurements, it was estimated that the fluorescence intensity of 1- and 2-PnA-PC is about 20% of that observed in egg PC vesicles (see Figure 2 and Table I). This is reflected in the shorter average fluorescence lifetime of PnA-PC bound to PC-TP as compared to vesicles (Table II). Sklar et al. (1977c) reported that the quantum yield of *trans*-PnA in single solvents is on the order of 10% of that measured for *trans*-PnA in dipalmitoyl-PC vesicles. This indicates that the relatively low quantum yield in PC-TP compares well with that observed for solvents. In agreement with the two chromophores present, diPnA-PC bound to PC-TP has double the fluorescence intensity of 1- and 2-PnA-PC but only 30% of the anticipated fluorescence intensity in egg PC vesicles (see Table I). The relatively low fluorescence intensity in vesicles must be ascribed to short-range interactions between the two polyene fatty acids on the same diPnA-PC molecule, leading to fluorescence quenching. Apparently, this short-range interaction does not take place when diPnA-PC is bound to PC-TP.

The PnA-containing phospholipids are very suitable probes for the investigation of membrane dynamics (Wolber & Hudson, 1981). It has the additional advantage that PnA is a natural fatty acid, thus minimally perturbing the system. This is also borne out by the biosynthetic incorporation of PnA into the phospholipids of *Escherichia coli* (Tecoma et al., 1977). To date, PnA has found only very limited use in the studies of protein–lipid interactions (Sklar et al., 1977b; Kimelman et al., 1979; Berde et al., 1979). In this paper, we show by measuring fluorescence anisotropy decay of 1-PnA-, 2-PnA-, and diPnA-PC bound to PC-TP that both the *sn*-1 and *sn*-2 fatty acyl chains are immobilized on the protein, i.e., have the rotational mobility of the protein. This is in full agreement with previous studies, where we measured the mobilities of spin-labeled probes bound at various positions along the *sn*-2 fatty acyl chain of PC upon incorporation into PC-TP (Devaux et al., 1977; Machida & Ohnishi, 1978). Despite the occurrence of two fluorescence lifetimes (see Table II), one rotational correlation time is obtained that reflects the immobilization of the probe. Under such conditions, the fluorescence lifetime components have the same anisotropy decay (Dale et al., 1977). The results in Table III show that *sn*-1- and *sn*-2-parinaroyl chains gave rise to different correlation times (26 and 11 ns, respectively). This can only be explained by assuming that both the *sn*-1 and *sn*-2 fatty acyl chains have their own distinct binding sites. This contention is supported by the differences in the main fluorescence lifetime component of 1-PnA- and 2-PnA-PC, i.e., 1.1 and 1.7 ns, respectively (see Table II). Independent of the shape of the protein, a parallel alignment of both fatty acyl chains should have given one correlation time. This not being so indicates that the two fatty acyl chains make a certain angle. The correlation time of 11 ns for the *sn*-2-parinaroyl chain is characteristic for a spherical globular protein of a molecular weight of 25 000, i.e., the molecular weight of PC-TP (Visser & Lee, 1982). On the other hand, the correlation time of 26 ns for the *sn*-1-parinaroyl chain indicates that PC-TP has to be elongated, i.e., nonspherical. The rotational frictional properties of prolate and oblate ellipsoids and the effect on fluorescence depolarization have been extensively investigated (Perrin, 1934; Weber, 1952; Tao, 1969). The apparent discrepancy of PC-TP being both spherical and nonspherical can be alleviated when we assume that the *sn*-1 fatty acyl chain is parallel to the long symmetry axis of a prolate ellipsoid and the *sn*-2 fatty acyl chain makes an angle of 60–90° (see Appendix). If this model holds true, the axial ratio of the ellipsoid can be estimated to be 2.5. The longest correlation time must be ascribed to the slowest rotation of the protein around the

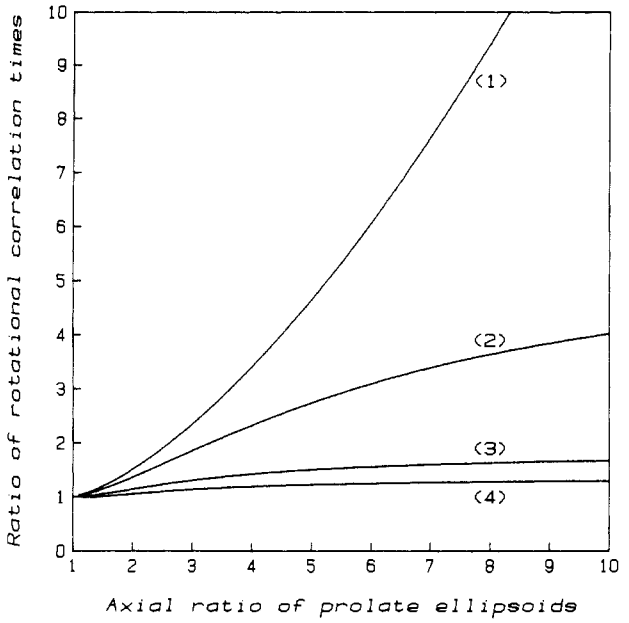


FIGURE 8: Ratio $\langle\phi\rangle/\phi$ of the average rotational correlation time of a prolate ellipsoid and that of an equivalent sphere as a function of the axial ratio of the ellipsoid ($\rho$). The four curves labeled 1–4 refer to an angle ($\theta$) of 0, 30, 60, and 90°, respectively, that the transition moment of the fluorophore makes with the main symmetry axis of the ellipsoid.

short semiaxis whereby the transition moment of the 1-PnA chromophore is oriented parallel to the long symmetry axis. The correlation time of bound diPnA-PC is 15 ns, which is the harmonic mean of the correlation times for 1-PnA- and 2-PnA-PC. This indicates that the orientation of the PC molecule on PC-TP is fixed such that, for example, the *sn*-1 fatty acyl chain cannot be accommodated by the binding site of the *sn*-2 fatty acyl chain.

In a recent study, photoactivable PC analogues containing carbene precursors on the *sn*-2 fatty acyl chain were used to probe the lipid binding site of PC-TP (Westerman et al., 1983). Evidence was provided that upon photolysis cross-linking occurred to Tyr-54 and the peptide segment $Val^{171}$-Phe-Met-Tyr-Phe-$Asp^{177}$. This peptide has a strongly predicted $\beta$-strand structure along with the *sn*-2 fatty acyl chain is presumed to be aligned. As for the moment, there is no information available on the chemical characteristics of the binding site of the *sn*-1 fatty acyl chain. Analysis of the coupling products of the bound photoreactive PC molecule showed that no cross-linking occurred between the *sn*-2 and *sn*-1 fatty acyl chain. This agrees with our spectroscopic evidence that both fatty acyl chains occupy different sites on PC-TP. This is the first example of a phospholipid–protein complex in which the two fatty acyl chains of the phospholipid are oriented in a nonparallel and strictly separated fashion. It is possible that this orientation is preeminent for the PC-TP to insert and extract PC molecules at phospholipid interfaces.

Acknowledgments

We are grateful to Dr. P. Somerharju for his advice and stimulating suggestions. We acknowledge the skillful assistance of C. van den Bergh and A. van Hoek.

Appendix

*Decay of Fluorescence Anisotropy for Prolate Ellipsoids.* The fluorescence anisotropy decay function for an irregularly shaped body has five exponential decay terms (Tao, 1969; Belford et al., 1972). The anisotropy decay function in the case of ellipsoids of revolution contains three correlation times ($\phi_1$, $\phi_2$, and $\phi_3$), which can be related to the diffusion coefficients ($D_\parallel$ and $D_\perp$) around the three axes of revolution (Perrin, 1934, 1936; Tao, 1969). $D_\parallel$ is the rotational diffusion coefficient around the main symmetry axis, and $D_\perp$ is the diffusion coefficient perpendicular to the main symmetry axis. Note that the two diffusion coefficients perpendicular to the main symmetry axis are degenerate. The correlation times of the triexponential function are

$$\phi_1 = (6D_\perp)^{-1} \tag{1a}$$

$$\phi_2 = (5D_\perp + D_\parallel)^{-1} \tag{1b}$$

$$\phi_3 = (2D_\perp + 4D_\parallel)^{-1} \tag{1c}$$

and the amplitudes are

$$a_1 = [(3/2)\cos^2\theta - 1/2]^2 \tag{2a}$$

$$a_2 = 3\cos^2\theta \sin^2\theta \tag{2b}$$

$$a_3 = (3/4)\sin^4\theta \tag{2c}$$

where $\theta$ is the angle between the transition moment of the fluorescent molecule and the symmetry axis of the ellipsoid. It is assumed that the absorption and emission dipoles are identical. A prolate ellipsoid is generated by rotating an ellipse around its long semiaxis, which is the main symmetry axis, and therefore has a rodlike shape. The disk-shaped, oblate ellipsoid is obtained by rotating the ellipse around its short semiaxis. The diffusion constants of prolate or oblate ellipsoids can be expressed in the isotropic diffusion constant ($D$) of a sphere of equivalent volume ($V$) and the axial ratio ($\rho$) of the ellipsoid ($\rho > 1$ for a prolate; $\rho < 1$ for an oblate). The rotational correlation time of sphere is given by

$$\phi = (6D)^{-1} = \eta V/(kT) \tag{3}$$

($\eta$ is viscosity and $T$ is temperature). If we restrict ourselves to prolate ellipsoids, the ratio of the three correlation times and that of an equivalent sphere becomes, respectively

$$\phi_1/\phi = 6[F_\perp(\rho)]^{-1} \tag{4a}$$

$$\phi_2/\phi = 6[F_\perp(\rho) + F_\parallel(\rho)]^{-1} \tag{4b}$$

$$\phi_3/\phi = 6[2F_\perp(\rho) + 4F_\parallel(\rho)]^{-1} \tag{4c}$$

where

$$F_\perp(\rho) = \frac{(3/2)\rho}{\rho^4 - 1}\left[\frac{2\rho^2 - 1}{(\rho^2 - 1)^{1/2}} \ln\left[\rho + (\rho^2 - 1)^{1/2}\right] - \rho\right] \tag{5a}$$

$$F_\parallel(\rho) = \frac{(3/2)\rho}{\rho^2 - 1}\left[\rho - \frac{\ln\left[\rho + (\rho^2 - 1)^{1/2}\right]}{(\rho^2 - 1)^{1/2}}\right] \tag{5b}$$

Since we have measured single correlation times, it is convenient to use an average correlation time $\langle\phi\rangle$ (Dale et al., 1977), which is a weighted harmonic mean of the individual correlation times $\phi_1$, $\phi_2$, and $\phi_3$:

$$\langle\phi\rangle = \sum_{i=1}^{3} a_i \left(\sum_{i=1}^{3} a_i/\phi_i\right)^{-1} \tag{6}$$

The amplitudes $a_i$ are dependent on the angle $\theta$ (eq 2a–c). The ratio $\langle\phi\rangle/\phi$ as a function of the axial ratio $\rho$ for four values of $\theta$ has been presented in Figure 8. By inspection of the curves we can arrive at several important conclusions. For arbitrary values of $\theta$ between 60 and 90° (curves 3 and 4, respectively), the average rotational correlation time of prolates is virtually identical with that of an equivalent sphere; only in the case of very elongated prolates ($\rho > 10$) is the correlation

time somewhat longer. The apparent rotation is considerably slower even at relatively small values of $\rho$ ($1 < \rho < 5$) when the transition moment of the fluorophore is exactly parallel to the main symmetry axis ($\theta = 0$; curve 1).

**Registry No.** 1-PnA-PC, 88496-02-0; diPnA-PC, 88547-62-0; GPC, 28319-77-9; 1-PnA-LPC, 88496-03-1; *cis*-parinaroyl anhydride, 72541-36-7; palmitoyl anhydride, 623-65-4.

## References


Akeroyd, R., Moonen, P., Westerman, J., Puyk, W. C., & Wirtz, K. W. A. (1981) *Eur. J. Biochem. 114*, 385–391.

Batzri, S., & Korn, E. D. (1973) *Biochim. Biophys. Acta 298*, 1015–1019.

Belford, G. G., Belford, R. L., & Weber, C. (1972) *Proc. Natl. Acad. Sci. U.S.A. 69*, 1392–1393.

Berde, C. B., Hudson, B. S., Simoni, R. D., & Sklar, L. A. (1979) *J. Biol. Chem. 254*, 391–400.

Bligh, E. G., & Dyer, W. J. (1959) *Can. J. Biochem. Physiol. 37*, 911–917.

Burstein, E. A., Vedenkina, N. S., & Ivkova, M. N. (1973) *Photochem. Photobiol. 18*, 263–279.

Dale, R. E., Chen, L. A., & Brand, L. (1977) *J. Biol. Chem. 252*, 7500–7510.

Davidson, F. M., & Long, C. (1958) *Biochem. J. 69*, 458–466.

Demel, R. A., Wirtz, K. W. A., Kamp, H. H., Geurts van Kessel, W. S. M., & van Deenen, L. L. M. (1973) *Nature (London), New Biol. 246*, 102–105.

Devaux, P. F., Moonen, P., Bienvenue, A., & Wirtz, K. W. A. (1977) *Proc. Natl. Acad. Sci. U.S.A. 74*, 1807–1810.

Gunstone, F. D., & Subbarao, R. (1967) *Chem. Phys. Lipids 1*, 349–359.

Gupta, C. M., Radhakrishnan, R., & Khorana, H. G. (1977) *Proc. Natl. Acad. Sci. U.S.A. 74*, 4315–4319.

Johnson, L. W., Hughes, M. E., & Zilversmit, D. B. (1975) *Biochim. Biophys. Acta 375*, 176–185.

Kamp, H. H., Wirtz, K. W. A., & van Deenen, L. L. M. (1973) *Biochim. Biophys. Acta 318*, 313–325.

Kamp, H. H., Sprengers, E. D., Westerman, J., Wirtz, K. W. A., & van Deenen, L. L. M. (1975) *Biochim. Biophys. Acta 398*, 415–423.

Kimelman, D., Tecoma, E. S., Wolber, P. K., Hudson, B. S., Wickner, W. T., & Simoni, R. D. (1979) *Biochemistry 18*, 5874–5880.

Machida, K., & Ohnishi, S. (1978) *Biochim. Biophys. Acta 507*, 156–164.

Moonen, P., Haagsman, H., van Deenen, L. L. M., & Wirtz, K. W. A. (1979) *Eur. J. Biochem. 99*, 439–445.

Papenhuijzen, J., & Visser, A. J. W. G. (1983) *Biophys. Chem. 17*, 57–65.

Perrin, F. (1934) *J. Phys. Radium 5*, 497–511.

Perrin, F. (1936) *J. Phys. Radium 7*, 1–11.

Rothman, J. E., & Dawidowicz, E. A. (1975) *Biochemistry 14*, 2809–2816.

Rouser, G., Fleischer, S., & Yamamoto, A. (1970) *Lipids 5*, 494–496.

Schroeder, F. (1983) *Eur. J. Biochem. 132*, 509–516.

Schroeder, F., Holland, J. F., & Vagelos, P. R. (1976) *J. Biol. Chem. 251*, 6739–6746.

Selinger, Z., & Lapidot, Y. (1966) *J. Lipid Res. 7*, 174–175.

Sklar, L. A., Hudson, B. S., & Simoni, R. D. (1975) *Proc. Natl. Acad. Sci. U.S.A. 72*, 1649–1653.

Sklar, L. A., Hudson, B. S., & Simoni, R. D. (1977a) *Biochemistry 16*, 819–828.

Sklar, L. A., Hudson, B. S., & Simoni, R. D. (1977b) *Biochemistry 16*, 5100–5108.

Sklar, L. A., Hudson, B. S., Petersen, M., & Diamond, J. (1977c) *Biochemistry 16*, 813–819.

Sklar, L. A., Miljanich, G. P., & Dratz, E. A. (1979) *Biochemistry 18*, 1707–1716.

Somerharju, P., Brockerhoff, H., & Wirtz, K. W. A. (1981) *Biochim. Biophys. Acta 649*, 521–528.

Somerharju, P., van Paridon, P., & Wirtz, K. W. A. (1983) *Biochim. Biophys. Acta 731*, 186–195.

Szabo, A. G., & Rayner, D. M. (1980) *J. Am. Chem. Soc. 102*, 554–563.

Tao, T. (1969) *Biopolymers 8*, 609–632.

Tecoma, E. S., Sklar, L. A., Simoni, R. D., & Hudson, B. S. (1977) *Biochemistry 16*, 829–835.

van den Bosch, H., & van Deenen, L. L. M. (1965) *Biochim. Biophys. Acta 106*, 326–337.

van Hoek, A., Vervoort, J., & Visser, A. J. W. G. (1983) *J. Biochem. Biophys. Methods 7*, 243–254.

Visser, A. J. W. G. (1982) *Biochim. Biophys. Acta 692*, 244–251.

Visser, A. J. W. G., & Lee, J. (1982) *Biochemistry 21*, 2218–2226.

Wahl, Ph. (1979) *Biophys. Chem. 10*, 91–104.

Waring, A. J., Glatz, P., & Vanderkooi, J. M. (1979) *Biochim. Biophys. Acta 557*, 391–398.

Weber, G. (1952) *Biochem. J. 51*, 145–155.

Welti, R., & Silbert, D. F. (1982) *Biochemistry 21*, 5685–5689.

Westerman, J., Wirtz, K. W. A., Berkhout, T., van Deenen, L. L. M., Radhakrishnan, R., & Khorana, H. G. (1983) *Eur. J. Biochem. 132*, 441–449.

Wirtz, K. W. A. (1982) in *Lipid-Protein Interactions* (Jost, P. C., & Griffith, O. H., Eds.) Vol. 1, pp 151–231, Wiley-Interscience, New York.

Wirtz, K. W. A., Vriend, G., & Westerman, J. (1979) *Eur. J. Biochem. 94*, 215–221.

Wolber, P. K., & Hudson, B. S. (1981) *Biochemistry 20*, 2800–2810.